PERGAMON

Journal of Quantitative Spectroscopy & Radiative Transfer 67 (2000) 169–180

Journal of Quantitative Spectroscopy & Radiative Transfer

www.elsevier.com/locate/jqsrt

Balloon-borne submillimeter observations of upper stratospheric O_2 and O_3

J.R. Pardo[a,b,*], L. Pagani[b], G. Olofsson[c], P. Febvre[d], J. Tauber[e]

[a]*Columbia University, NASA-Goddard Institute for Space Studies, 2880 Broadway, NY 10025, New York, USA*
[b]*DEMIRM, URA 336 du CNRS, Observatoire de Paris-Meudon, 61 Avenue de l'Observatoire, 75014 Paris, France*
[c]*Stockholm Observatory, SE-133 36 Saltsjöbaden, Sweden*
[d]*LAHC, Université de Savoie, 7336 Le Bourget du Lac Cedex, France*
[e]*ESA, Astrophysics Division, Space Science Department, ESTEC, P.O. Box 299, 2200 AG Noordwijk, Netherlands*

Received 4 September 1998

Abstract

A Swedish–French submillimeter telescope consisting on a 60 cm diameter Cassegrain telescope with a liquid helium cooled supraconductor–isolator–supraconductor (SIS) heterodyne receiver flew on September 25th 1997 in the southwest of France. It was carried out by the Pointed InfraRed Observation Gondola (PIROG, 8th flight) to a ceiling altitude of about 39.5 km. The submillimeter thermal emission of molecular oxygen ($N_J = 3_2 \rightarrow 1_2$ rotational resonance at 424.7631 GHz) and ozone (lines: $24_{1,23} \rightarrow 24_{0,24}$ at 424.846 GHz, $28_{2,26} \rightarrow 27_{3,25}$ at 425.158 GHz and $17_{1,17} \rightarrow 16_{0,16}$ at 441.340 GHz) was collected during about 8.5 h. These are the first submillimeter high-resolution observations of molecules in the middle atmosphere obtained by a non-ground-based instrument and will be helpful in preparing future submillimeter limb-sounding missions, like *EOS-MLS* (NASA) and *Odin* (Swedish Space Corporation). We present in this paper the calibration of the atmospheric data and their analysis along with some discussions on ozone mixing ratio just above the ceiling altitude of the experiment. Some validations of our results are done by means of comparisons with temperatures and ozone mixing ratios obtained simultaneously at the Observatoire de Haute Provence (OHP) Lidar station, located also in Southern France. The radiative transfer code used in this work to fit the data and retrieve temperature, pressure and ozone mixing ratio has been developed for the *Odin* mission. This work is an effective test of such a software package.

* Corresponding author. Present address: George W. Downs Laboratory of Physics, California Institute of Technology, MS 320-47, Pasadena, California 91125, USA. Tel.: 1-626-3956664; fax: 1-626-7968806.

0022-4073/00/$ - see front matter
PII: S0022-4073(99)00232-0

1. Introduction

Ozone and molecular oxygen are important molecules for terrestrial life. While the former is at the center of modern research on the physics and chemistry of the atmosphere, the second is a perfect tool to derive vertical temperature/pressure atmospheric profiles by means of microwave spectroscopic observations because its stratospheric mixing ratio is very well known [1]. Ozone is an important gas in the mechanisms that govern the temperature profile of the stratosphere. In this atmospheric region it is also the main agent stopping the solar UV in the wavelength domain $\sim$200–300 nm due to photodissociation processes.

The microwave resonant thermal emission of atmospheric O_2 is due to a permanent magnetic dipole moment in its ground electronic state coming from two parallel electron spins. The dipole moment is equal to 2 Böhr magnetons (0.0186 Debyes). It gives rise to a spin-rotation spectrum composed by a cluster of lines around 60 GHz and isolated lines at 118.75, 424.76 GHz and at other different frequencies in the submillimeter region. Details about this spectrum can be found elsewhere [2–4]. In the atmosphere, the "dry" microwave absorption has also contributions due to the non-resonant Debye spectrum of O_2 below 10 GHz, pressure-induced nitrogen absorption [5] as well as resonant absorption by trace gases (ozone, N_2O, CO, SO_2, isotopic and vibrationally species of O_2,O_3, etc.). The H_2O absorption is highly variable in the troposphere and it is the main factor limiting ground-based observations of both astrophysical sources or stratospheric species in the millimeter and, more dramatically, in the submillimeter region. Ground-based millimeter-wave spectroscopic observations of minor atmospheric gases have been carried out since the early 1980s [6]. These measurements have been shown as a useful technique because they do not depend on sunlight and are not significantly affected by aerosols. They are also a good help to validate satellite datasets and the cost is low compared with balloon-borne or satellite experiments. But the technique has some inherent disadvantages: only local information is retrieved with a rather poor vertical resolution (limited to about the value of the pressure scale height, see [7]). These drawbacks can be avoided by making use of a limb-sounding instrument on board of a satellite (see a general overview of the technique in [8]). It provides access to large zones of our planet and to vertical domains mainly limited by the technical characteristics of the system (spectral resolution and coverage, satellite and scanning velocities, etc.). Limb-sounding avoids tropospheric absorption when studying stratospheric–mesospheric species and provides access to a much better vertical resolution. The microwave limb sounding technique has been already operated by the Microwave Limb Sounder (MLS) on the Upper Atmosphere Research Satellite (UARS). All the detectors were in the millimeter-wave range in this case (around 60, 183 and 205 GHz). The new generation MLS (scheduled for 2002 on the Earth Observing System [EOS]) will use submillimeter-wave receivers making profit of the fact that submillimeter lines of several trace gases of interest are in general stronger than their millimeter lines. In some cases (HCl for instance) the resonances begin in the submillimeter region only. In addition, the antenna beam will be narrower for a given antenna size, and this fact intrinsically helps to reach better vertical resolution. Other satellite projects will make use of submillimeter instruments for limb-sounding measurements of upper atmospheric species (*Odin*, a Swedish Small Project for Astronomical and Atmospheric Research, see [9]) and submillimeter astronomy (Submillimeter Wave Astronomy Satellite [SWAS], and also *Odin*).

Balloon-borne instruments have a low cost compared to satellites and can provide access to observing conditions for submillimeter astronomy and aeronomy that avoid tropospheric

absorption. We will present in this paper a set of atmospheric submillimeter spectra of O_2 and O_3 obtained with the submillimeter telescope described below. It is the first non-ground-based experiment to obtain submillimeter data of these two atmospheric species in the upper stratosphere and lower mesosphere while from the ground, submillimeter detections of O_2,O_3 and isotopic and vibrationally excited H_2O species have been recently reported [10] (see Table 1).

The data have been analyzed to serve several purposes. First, 424 GHz spectra of O_2 have been deconvolved to retrieve the atmospheric temperature and pressure in the first few kilometers above the ceiling level of the gondola. Then, two O_3 lines observed simultaneously in the two bands of the submillimeter receiver could be fitted in order to retrieve the relative gain of these two bands. A selected set of combined O_2 and O_3 spectra allowed us to estimate the forward efficiency of the telescope during the experiment. Finally, 110 individual O_3 spectra with typical rms errors of 0.3 K were recorded during a total of 7 h and were used to retrieve stratospheric O_3 mixing ratios in Southern France. The obtained spectra also allowed us to test a spectroscopic inversion software package intended for application to *Odin* data.

In Section 2 we present a description of the observation procedure. The receiver itself has been presented elsewhere [11]. Some details about the radiative transfer theory used in this work are given in Section 3. The analysis of the data is described in Section 4. The results are presented and discussed in Section 5. We summarize our conclusions in Section 6.

2. Observations

The main scientific goal of this experiment was to detect molecular oxygen in selected giant molecular clouds of our Galaxy (for further details on the results of the PIROG-8 astrophysical observations, see [12]). At around 39 km of altitude the strong atmospheric $^{16}O_2$ lines are narrow

Table 1
Spectroscopic parameters of the O_2 and O_3 rotational resonances reported in this work. J, K_a K_b are rotational quantum numbers used to describe the rotational energy levels of an asymmetric top molecule whereas N, J are the quantum numbers to describe the spin-rotation spectrum of molecular oxygen (see [13]). The other spectroscopic parameters are introduced in Section 3

Ozone: $\|\boldsymbol{\mu}\| = 0.5337$ Debyes, $Q = 0.6497285T^{3/2}$						
$J_{K_aK_b}$	$J'_{K'_aK'_b}$	v_c (GHz)	Line strength	E_{lower} (K)	γ (300 K) (MHz/mb)	Temperature exponent (x)
$24_{1\ 23}$	$24_{0\ 24}$	424.84594	8.15	353.2	2.23	0.72
$28_{2\ 26}$	$27_{3\ 25}$	425.15777	6.95	498.2	2.18	0.72
$17_{1\ 17}$	$16_{0\ 16}$	441.34037	12.4	161.9	2.19	0.72
$^{16}O_2$: $\|\boldsymbol{\mu}\| = 2\mu_{\text{Bohr}} = 0.0186$ Debyes, $Q = 0.7332246T$						
N_J	$N'_{J'}$	v_c (GHz)	Line strength	E_{lower} (K)	Δv_0 (MHz/mb)	Temperature exponent (x)
3_2	1_2	424.76312	0.392	4.0	1.93	0.2

enough to allow some significant transmission at the Doppler-shifted position of the same resonances in selected astrophysical sources. The PIROG gondola was carrying a 60 cm Cassegrain Telescope equipped with a 425/441 GHz SIS heterodyne receiver followed by a 400 channel autocorrelation spectrometer providing frequency resolutions ranging from 800 to 50 kHz. In the lowest-resolution mode the whole atmospheric O_2 line at 424.7631 GHz along with an ozone line at 424.8459 are covered simultaneously. The atmospheric O_2 line is used to derive temperature and pressure at the ceiling position (see below). Due to its proximity to the Doppler-shifted position of the O_2 resonance in one of the astrophysical sources, the 424.8459 GHz atmospheric ozone line was tracked by the experiment in the high-resolution mode during several hours, allowing to follow the evolution of upper stratospheric ozone signal from sunrise to 14:00 UT approximately.

The double-side band (DSB) receiver noise temperature (T_{sys}) was measured at ambient pressure in the laboratory before and after integration of the receiver on the gondola. The mean values of DSB T_{sys} within the bandwidth of the spectrometer were around 270 K. According to these measurements a DSB T_{sys} of 200 K was expected at ceiling altitude where the liquid Helium temperature is about 1.5 K instead of 4.3 K at laboratory but because of electrical perturbations on the SIS junction, the actual sensitivity was only 240 K [11].

The calibration procedure is as follows: two internal loads at ambient (typically 260 K) and hot (typically 320 K) were introduced in the beam and measured. The ratio of the two output powers then gives the receiver sensitivity. Because of a bad thermalization of the hot load (a negative correction of 9 to 12 K was to be applied to the thermocouple measurement), we also used the cold sky (3 K cosmic background radiation far away from the O_2 line) as a cold load to cross-check our values. We tried to measure the telescope forward efficiency (η_f) by executing a 'skydip' (a measurement of the sky brightness at different elevations) but baseline instabilities precluded the possibility to measure this value which we however estimated to be $\eta_f \approx 0.95$ and most probably above 0.9. Another step of the calibration has been to estimate the sideband ratio, the receiver being sensitive to both Upper and Lower sidebands. This is discussed further below (see Section 4.1).

3. Radiative transfer

To analyze the observations presented in this paper we can use a polarization independent radiative transfer equation without considering scattering mechanisms nor refraction. The radiative transfer equation for the specific intensity (I) of the radiation is thus a relatively simple differential scalar equation that we can write as follows:

$$\frac{\mathrm{d}I(\mathbf{r},\mathbf{n},\nu)}{\mathrm{d}s} = \varepsilon_\nu - \kappa_\nu I(\mathbf{r},\mathbf{n},\nu), \tag{1}$$

where $\varepsilon_\nu \mathrm{d}w\,\mathrm{d}\nu\,\mathrm{d}s\,\mathrm{d}\sigma$ and $\kappa_\nu I(\mathbf{r},\mathbf{n},\nu)\mathrm{d}w\,\mathrm{d}\nu\,\mathrm{d}\sigma\,\mathrm{d}s$ are the amounts of energy emitted and absorbed at frequency ν in a pencil of solid angle $\mathrm{d}w$ in the direction $\mathbf{r}$ trough a cylinder of length $\mathrm{d}s$ and section $\mathrm{d}\boldsymbol{\sigma} = \mathrm{d}\sigma\mathbf{n}$. In this definition ε_ν and κ_ν are the absorption and emission coefficients. After rearranging and considering the problem as a 1-D one in the direction of $\mathbf{r}$ we can write [under local

thermodynamic equilibrium (LTE), see below] the very simple equation:

$$\frac{\mathrm{d}I_\nu(s')}{\mathrm{d}\tau_\nu} = -I_\nu(s') + S_\nu(T), \tag{2}$$

where s' is a coordinate along the path, $S_\nu = \varepsilon_\nu/\kappa_\nu$ is the so-called source function, and $\mathrm{d}\tau_\nu = \kappa_\nu\,\mathrm{d}s$ is the differential opacity. The solution of this equation can be easily given in an integral form

$$I_\nu(s) = I_\nu(0)\mathrm{e}^{-\tau_\nu(0,s)} + \int_0^s S_\nu(s')\mathrm{e}^{-\tau_\nu(s',s)}\kappa_\nu(s')\,\mathrm{d}s'. \tag{3}$$

As we will see below only radiation originated within the vertical domain from the ceiling altitude of the balloon to 10 or 15 km above it is contributing to the measured atmospheric signal. Typical temperatures and pressures in that region can range from $\sim$220 to 320 K and $\sim$2.5 to 0.5 mb, respectively. These physical conditions allow to assume that thermodynamic properties in a small volume of atmospheric gas are fully controlled by the local physical temperature T. This assumption is known as the local thermodynamic equilibrium (LTE) and one of its consequences (see [14]) is that the source function ($S_\nu = \varepsilon_\nu/\kappa_\nu$) equals to the Planck function $B_\nu(T) = 2h\nu^3/[c^2(\mathrm{e}^{h\nu/kT} - 1)]$, T being the physical temperature of the layer. In addition, a Planck's source function is the consequence of Boltzmann's law for the population of molecules in the available energy levels.

There are different ways to assign a temperature to the output radiance (in W/m/ster/cm) from the atmospheric path. The most general one is to assume that the output radiance at a given frequency is equal to that of a blackbody at temperature T_{EBB} (equivalent blackbody temperature). Simply by inverting the Planck function we obtain

$$T_{\mathrm{EBB}} = \frac{h\nu}{k(\ln(2h\nu^3/Ic^2) + 1)} = \frac{h\nu}{k(\ln(h\nu/kT_{\mathrm{RJ}}) + 1)}, \tag{4}$$

where the T_{RJ} is the temperature derived when making a Rayleigh–Jeans approximation to the equivalent blackbody at frequency ν prior to invert:

$$T_{\mathrm{RJ}} = \frac{c^2 I}{2K\nu^2}. \tag{5}$$

We can relate T_{EBB} and T_{RJ}:

$$T_{\mathrm{EBB}} = T_{\mathrm{RJ}} + \frac{h\nu}{2k} - \frac{h^2\nu^2}{3k^2 T_{\mathrm{RJ}}} + \cdots, \tag{6}$$

so the difference between T_{EBB} and T_{RJ} is, to the first order, a constant that depends on ν. The value of such a constant at 425 GHz is 10.2 K. Calibration procedures assuming the Rayleigh–Jeans approximation work reasonably well even at frequencies where the Rayleigh–Jeans approximation is in itself not valid because they rely upon the offset cancellation.

To analyze our measurements we should compare them with T_{RJ} from a radiative transfer code. We use Eq. (3) and calculate the absorption coefficient from oxygen and ozone lines layer by layer according to the following expression (see, for instance [15]):

$$(\kappa_{\nu_{lu}}) = \frac{8\pi^3 N\nu}{3hcQ}(\mathrm{e}^{-E_l/kT} - \mathrm{e}^{-E_u/kT}) \cdot S_{lu}|\boldsymbol{\mu}|^2 f(\nu, \nu_{u\leftarrow l}), \tag{7}$$

where v_{lu} is the central frequency of the transition between energy levels E_l and E_u, Q is the partition function and μ the dipole moment, S_{lu} is a non-dimensional parameter called line strength directly related with the transition probability. Finally $f(v, v_{lu})$ is the line shape function. This shape is dominated by collisions in the altitude domain 39–50 km. Consequently, we use a Van Vleck–Weisskopf line shape [4] with a half-width (γ) described by the power law:

$$\gamma(T) = \gamma(T_0) \cdot (T_0/T)^x. \tag{8}$$

The values of the spectroscopic parameters that we have used in our analysis are listed in Table 2. γ and x come from Liebe et al. [16] for O_2 and Barbe et al. [17] (x) and HITRAN-92 [18] (γ) for O_3.

The software package used in the analysis of the data is an improved version of that already used by the authors in previous works [19,20].

4. Data analysis

Due to the size of the balloon in the stratosphere (46 m of radius) the telescope can observe only at a maximum elevation of 60°. In order to determine the atmospheric layers that contribute to the signal measured by the instrument we have calculated the weighting function ($W_{v,\theta}$) versus frequency near the telluric O_2 resonance at elevation $\theta = 30°$ for the U.S. 1976 Stnd. Atm. Midlatitude Winter [21]. The weighting function is defined as follows:

$$W_{v,\theta}(z) = \frac{\partial \Gamma_{z\to\infty}(v,\theta)}{\partial z}, \tag{9}$$

where $\Gamma_{z\to\infty}(v,\theta)$ is the atmospheric transmission between z and the top of the atmosphere at frequency v and elevation θ. The results are shown in Fig. 1. From these calculations we have established the strategy to fit the spectra and retrieve physical parameters of the atmosphere (see Section 4.2).

4.1. Determination of the sideband ratio

Very important to obtain accurate atmospheric information from our spectroscopic measurements is the determination of the side band ratio of the receiver. To achieve that goal it has been proposed [22] to tune the receiver to observe two atmospheric ozone lines within the spectrometer range (see Table 1), one in each sideband, the intensity ratio of them being well known in the range of prevailing temperatures in the atmospheric region just above the position of the telescope. The tunability of the local oscillator allowed the observation of two ozone lines at central frequencies 425.1578 and 441.3404 GHz. Fitting the observed spectra (one of them is shown in Fig. 2, left) for different sideband ratios with our radiative transfer model yields a best fit ratio of ≈ 1.2–1.25. However, when tuned back to the O_2 frequency we found that the saturated O_2 telluric line measurement was too low to match the expected value when using a sideband ratio of 1.2 and that it was better explained with a ratio of 1. In that case the fit of the spectrum shown in the right part of Fig. 2 provides values of pressure and temperature at ceiling of 2.8 mb and 240 K (this value is quite consistent with an air temperature in the range of -30–35°C measured when the balloon

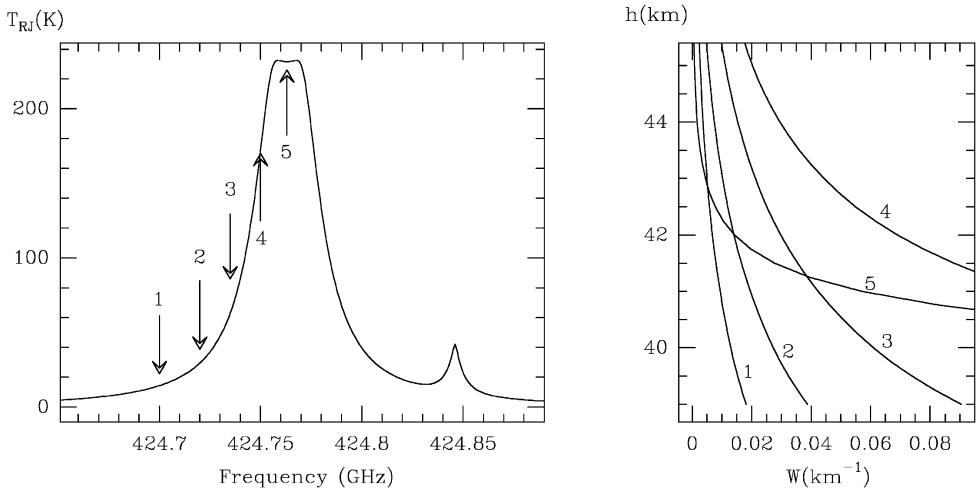

Fig. 1. Left: Simulated atmospheric spectrum between frequencies 424.651 and 424.89 GHz for the U.S. 1996 Stnd. Atm. Midlatitude Winter [21] and two air masses. The arrows indicate the positions of five individual frequencies for which the weighting function (defined in Eq. (9)) has been calculated (shown on the right).

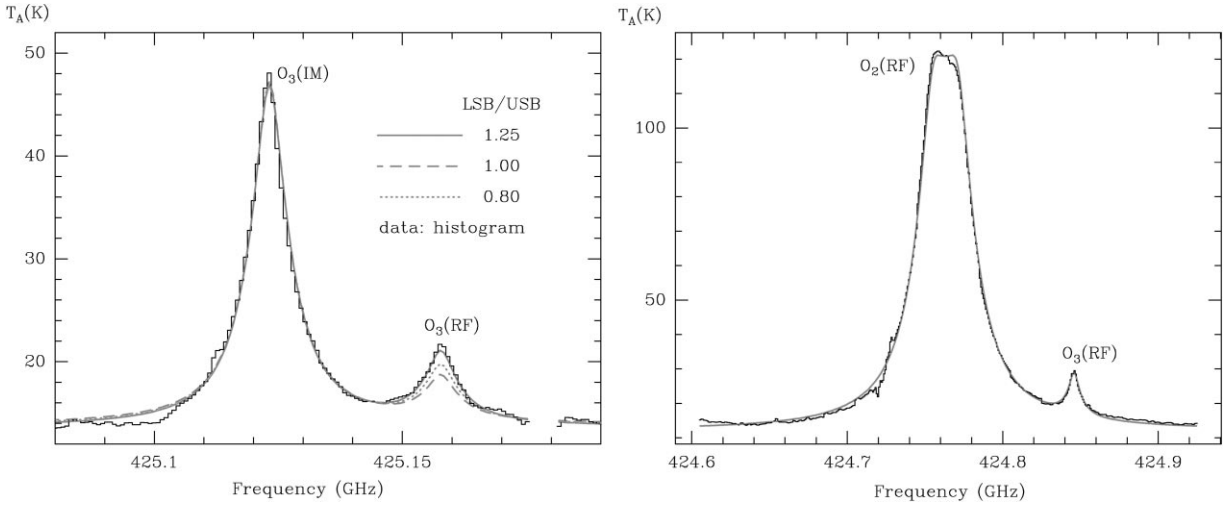

Fig. 2. Left: Spectrum obtained by the PIROG 8 experiment used to determine the sideband ratio of the receiver. Best fit is for LSB/USB ratio of 1.25; Right: Spectrum showing the telluric O_2 line at 425 GHz along with an O_3 line on its wing at 30° elevation. The fit of this spectrum provides T and P at ceiling along with ozone column density above the telescope.

reached the ceiling altitude, but also with lidar measurements performed at Observatoire de Haute Provence almost simultaneously, see below). Nevertheless, we have no direct evidence of the receiver sideband gain ratio changing with frequency because there is no measurable O_3 line in the upper side band when the local oscillator is tuned to observe the O_2 line but this remains the best explanation we can think of presently.

4.2. O_2 observations

At the beginning of the flight and at the end of it, several spectra of the 424.76 GHz telluric resonance were taken with a frequency coverage of 320 MHz. Using a sideband ratio of 1 and a forward (sky) efficiency of 0.95, and taking into account the analysis shown in Fig. 1, we have decided to fit these spectra using 20 km of atmosphere above the telescope position (with a "nominal" position of the stratopause at 49 km for the a priori atmospheric profile) and a set of free parameters described below. Temperature within the first 2 km above the telescope is accurately determined by the saturated signal of the central 10 MHz of the O_2 resonance (see Fig. 1). The pressure profile up to the stratopause (39–49 km) is calculated by our code from the signal in the wings of the line. Then, temperature up to the stratopause can also be given since the hydrostatic equilibrium and the equation of gases yield:

$$\mathrm{d}p = -g\rho\,\mathrm{d}z, \qquad p = \rho RT/M_{\mathrm{air}} \Rightarrow T = -Mg\Big/\left(R\frac{\partial \ln p}{\partial z}\right), \tag{10}$$

where M_{air} is the mean molar mass of the air, g is the local acceleration of gravity and R the ideal gas constant. Pressures and temperatures beyond the stratopause are then extrapolated.

In our analysis we have also introduced an extra free parameter for the total column density of O_3 in order to fit the resonance of this gas that appears at 424.85 GHz.

The spectra show an offset that is due to a spill-over contribution to the the signal. This offset is fitted by a spill-over temperature (free parameter, completely decoupled from the other three) multiplied by 0.05 ($=1-\eta_f$).

4.3. O_3 observations

During most of the flight, the autocorrelation spectrometer was used in a 200 kHz resolution mode. It was possible to record a total of 110 O_3 spectra at 424.85 GHz. The O_3 signal lies on the wing of O_2 emission so the data were fitted by using the average temperature profile derived from the analysis of O_2 as fixed information (240.5 K at the ceiling position of the instrument) and two free parameters, one for the pressure in order to fit this O_2 "baseline" and another one for the total column density of ozone.

5. Results and discussions

The experiment PIROG-8 was designed for observations of O_2 in Galactic giant molecular clouds. To accurately calibrate the astrophysical signal (or its absence), the fit of the atmospheric line is necessary to estimate the sky opacity. This has been an additional motivation for analyzing the atmospheric spectra.

Several spectra obtained at different elevations and their corresponding fits are shown in Fig. 3. Spectra on the left panel have a typical rms error of 1.3 K for an integration time of 5 s. Spectra on the right (O_3 line alone) present ~ 0.35 K rms for 25 s of integration time.

Temperatures and pressures derived by the inversion code (using a sideband ratio of 1 as stated above) at the beginning of the flight (7:00–7:40 UT) are the following: 240.5 ± 2.3 K and

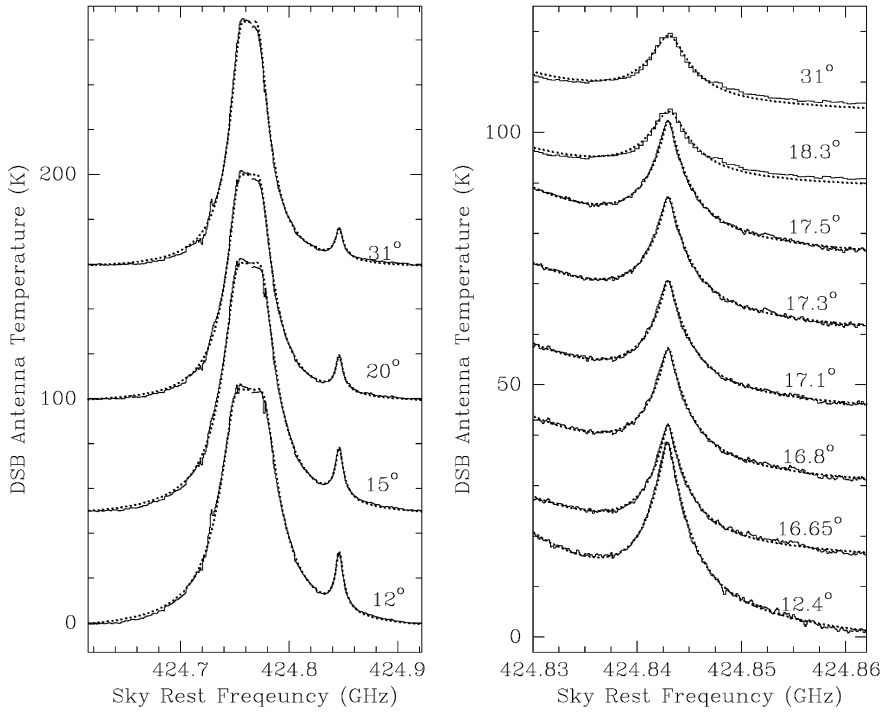

Fig. 3. O_2 and O_3 submillimetric spectra recorded during the PIROG-8 flight (dark histograms). Y-axis units are DSB antenna temperatures. The different spectra in the figure and their corresponding fits are shown after introducing artificial offsets of 50 K between spectra on the left panel and 15 K between spectra on the right panel. The fits obtained by our radiative transfer code are the solid grey lines. From these fits we obtain the temperature, pressure and ozone column density from the telescope position to the stratopause (the first two by assuming a lapse rate and a scale height from a standard atmosphere).

3.08 ± 0.05 mb. The value of the temperature is in a good agreement with upper mesospheric temperatures expected in midlatitudes during the fall. The lidar station at Observatoire de Haute Provence (OHP) located within less than 200 km from where most of the PIROG-8 flight took place provided us with a value of the temperature at 39 km of 244.09 ± 0.17 K that we can consider in a reasonable good agreement with our results. The mean value of O_3 mixing ratio recorded during this part of the flight was 7.5 ppmv at 39.5 km, or a column density of $3.17 \pm 0.06 \times 10^{17}$ molecules/cm^2.

The value $T = 240.5$ K was fixed for O_3 retrievals after 8:00 UT. The retrieved pressures at ceiling altitude and O_3 column densities during the whole flight are shown in Fig. 4. It is interesting to note that even though the pressure was only retrieved from the "baseline" (that is a small portion of the O_2 line wing) of ozone spectra during most of the flight the values found are well within 3 ± 0.2 mb.

In the middle atmosphere odd oxygen species O and O_3 interchange rapidly. The partitioning of O and O_3 is essentially under control of the following reactions:

$$O_3 + h\nu \rightarrow O_2(^3\Sigma_g^-) + O(^3P), \tag{11}$$

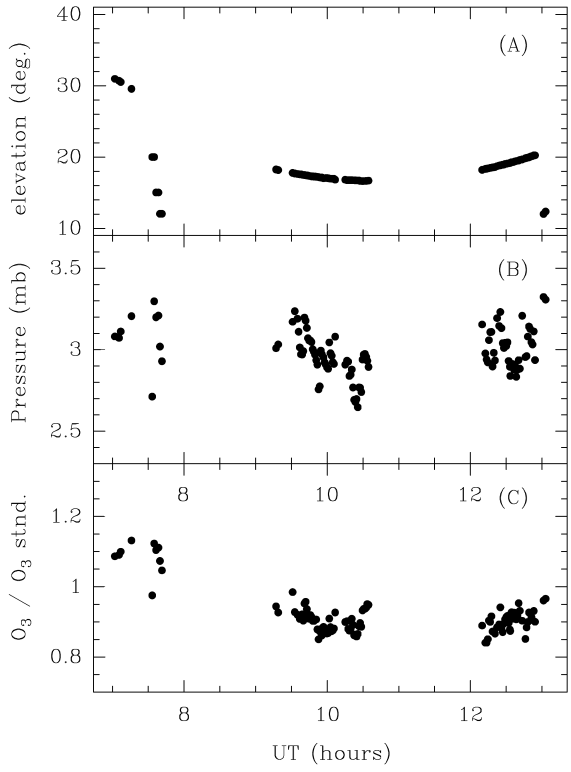

Fig. 4. (A) Elevations at which we have recorded O_3 atmospheric spectra during the PIROG-8 flight (versus universal time). (B) Average pressure at ceiling derived from fitting the "baseline" from which the O_3 emission emerges. (C) Ratio between Ozone column density derived from the fit and the one given by US 1996 Stnd. Atm. [21].

$$O_3 + h\nu \rightarrow O_2(^1\Delta_g) + O(^1D), \tag{12}$$

$$O + O_2 + M \rightarrow O_3 + M. \tag{13}$$

At the level of the stratopause O_3 is at least 10 times more abundant than O atoms so the conversion of O to O_3 during the night is a minor perturbation to the ozone mixing ratio. At 39.5 km ($\sim$ 10–12 km below the stratopause) we do not expect to see any notable change in the O_3 density. But our signal has a non negligible contribution from altitudes above the stratopause. At 39 km and for two air masses the opacity at 424.846 GHz is around 0.15 for a T_{RJ} of 40 K. From radiative transfer simulations we estimate that a contribution of 5 K at that frequency is due to ozone molecules located above 55 km ($\sim$2 scale heights from 39 km) and as much as 11 K is due to molecules above 50 km. Ozone mixing ratios are typically $\sim$7 ppmv at 39 km and go down to $\sim$1.5 ppmv at 55 km. The geometry of our observation does not provide a vertical resolution to separate these informations so we have decided to show our results in terms of ratio between retrieved O_3 column density and the one corresponding to the US 1976 Standard Atm. [21] corrected for the slight difference in pressure retrieved from each individual spectrum. Those results are shown in Fig. 4. The O_3 column densities found at the beginning of the flight (during dawn) are

clearly higher than those found at around 10:00 UT and 13:00 UT. A standard O_3 column density of $10^{17}\,cm^{-2}$ is expected above 50 km of altitude and it is diurnally variable to some extent. Models give a 18% variation at 54 km [23] and previous measurements are consistent with variations ranging from $\sim$13 to 30% [24,25]. The transition time from nighttime values to daytime values is $\sim$2 h at 50 km so the effect we see is probably real although unfortunately the experiment did not record any spectrum during the night to give more confidence to this conclusion.

The lidar station at OHP also provided us with some O_3 data up to an altitude of ~ 45 *km*, that in part validate our results. For two consecutive nights (September 25th and 26th) the results at OHP for 39.47 ± 4.1 km of altitude where 6.87×10^{11} and $6.91 \times 10^{11}\,cm^{-3}$, respectively, with error bars of 9.7%. Our retrievals are compatible with a mean value of the ozone density of $6.5 \times 10^{11}\,cm^{-3}$ at the level 3.08 mb, that is within the error bar of the OHP results.

6. Summary and conclusions

We have reported in this paper the first non-ground-based submillimeter heterodyne observations of atmospheric molecules. The data were obtained as part of a mission called PIROG-8 aiming at the observation of $^{16}O_2$ in selected Galactic giant molecular clouds. The data constitute a step in the preparation of submillimeter limb-sounding missions that will follow in the coming years the path opened by the millimeter mission *UARS-MLS*. An atmospheric retrieval software package under development for the *Odin* mission has been successfully tested in real submillimeter observation conditions owing to the PIROG-8 data providing extremely good fits. The atmospheric signal from two other ozone resonances separated by 16 GHz has been used to measure the value of the side band ratio of the receiver at that frequency. Pressures and temperatures at the ceiling position of the balloon were retrieved from the O_2 signal and were in good agreement with expected values and even with air temperatures measured by on board instruments (the direct measurement of temperature at 3 mb of pressure is rather difficult) and lidar measurements carried out at Observatoire de Haute Provence. O_3 column densities above ceiling were monitored during 7 h using an ozone resonance at 424.846 GHz. The results show in part the diurnal variation of O_3 concentration in the mesosphere and are in general in good agreement with simultaneous lidar measurements and typical mid-latitude ozone profiles in the upper stratosphere and in the mesosphere.

Acknowledgements

J.R. Pardo gratefully acknowledges additional financial support from the *NASA-Goddard Institute for Space Studies*, the *Observatoire de Paris-Meudon*, *CNES* and *Météo-France* for the development of this work. We want to thank all the technical people who made this flight a success and also the CNES launch team who turned our 4 h flight promise into a 8 h real flight. S. Godin and A. Hauchecorne from the French *Service d'Aéronomie* kindly provided us with the lidar ozone and temperature data from Haute Provence, which is gratefully acknowledged. The Swedish participation was financed by grants from the Swedish National Space Board.

References

[1] Fishbein EF et al. J Geophys Res 1996;101-D6:9983–10016.
[2] Tinkham M, Strandberg MW. Phys Rev 1955;97:937.
[3] Tinkham M, Strandberg MW. Phys Rev 1955;97:951.
[4] Rosenkranz PW. Absorption of microwaves by atmospheric gases. In: Janssen MA, editor. Atmospheric remote sensing by microwave radiometry. New York: Wiley, 1993.
[5] Liebe HJ. Int J Infrared Millimeter Waves 1989;10:631–50.
[6] Wilson WJ, Schwartz PR. J Geophys Res 1981;86-C:7385–8.
[7] Bevilacqua RM, Olivero JJ. J Geophys Res 1988;93-D8:9463–75.
[8] Waters JW. Limb sounding. In: Janssen MA, editor. Atmospheric remote sensing by microwave radiometry. New York: Wiley, 1993.
[9] von Schéele F. The Swedish Odin satellite to eye heaven and earth. Swedish Space Corporation Report (http://www.ssc.se/ssd/papers/odeye/odeye.html), 1996.
[10] Serabyn E, Weisstein EW, Lis DC, Pardo JR. Appl Opt 1998;37(12):2185–98.
[11] Deschamps A et al. A balloon experiment searching for the 425 GHz O_2 line with an SIS Receiver. Proceeding of the ESA Workshop on Millimeter Wave Technology and Applications, Espoo, Finland, May 1998.
[12] Ologson G et al. Astron Astrophys 1998; L81–L84.
[13] Gordy W, Cook RL. Microwave molecular spectra. New York: Wiley, 1984.
[14] Chandrasekhar S. Radiative transfer. Oxford: Oxford University Press, 1960.
[15] Kroto HW. Molecular rotation spectra. New York: Wiley, 1975, p. 67.
[16] Liebe HJ, Hufford GA, Cotton MG. Propagation modeling of moist air and suspended water/ice particles at frequencies below 1000 GHz. AGARD 52nd Specialists' Meeting of the Electromagnetic Wave Propagation Panel, Palma de Mallorca (Spain), 1993.
[17] Barbe A, Regalia L, Plateaux JJ, Von Der Heyden P, Thomas X. J Mol Spec 1996;180:175–82.
[18] Rothman LS et al. JQSRT 1992;48:469–507.
[19] Pardo JR, Cernicharo J, Lellouch E, Paubert G. J Geophys Res 1996;101-D22:28,723–30.
[20] Pardo JR, Cernicharo J, Pagani L. J Geophys Res 1998;103–D6:6189–202.
[21] U.S. Commitee On Extension to the Stnd. Atm. U.S. Printing Office, Washington D.C., 1976.
[22] Cernicharo J. Thèse de doctorat d'État, Paris VI University, 1988.
[23] Vaughan G. Q J R Meteorol Soc 1984;110:239–60.
[24] Lobsiger E, Künzi KF. J Atmos Terr Phys 1986;48:1153–8.
[25] Ricaud P, Brillet J, de La Noë J, Parisot JP. J Geophys Res 1991;96-D:18,617–29.